ISSN 1674-1056
http://cpb.iphy.ac.cn
http://iopscience.iop.org/cpb
中国物理 B
Chinese Physics
中国物理 Chinese Physics B

Probing conformational change of T7 RNA polymerase and DNA complex by solid-state nanopores

Xin Tong(童鑫), Rui Hu(胡蕊), Xiaoqing Li(李晓晴), Qing Zhao(赵清)

Citation: Chin. Phys. B . 2018, 27(11): 118705. **doi:** 10.1088/1674-1056/27/118705
Journal homepage: http://cpb.iphy.ac.cn; http://iopscience.iop.org/cpb

What follows is a list of articles you may be interested in

Interaction between human telomeric G-quadruplexes characterized by single molecule magnetic tweezers

Yi-Zhou Wang(王一舟), Xi-Miao Hou(侯锡苗), Hai-Peng Ju(车海鹏), Xue Xiao(肖雪), Xu-Guang Xi(奚绪光), Shuo-Xing Dou(窦硕星), Peng-Ye Wang(王鹏业), Wei Li(李伟)

Chin. Phys. B . 2018, 27(6): 068701. **doi:** 10.1088/1674-1056/27/6/068701

Improved data analysis method of single-molecule experiments based on probability optimization

Weili Zhai(翟伟利), Guohua Yuan(袁国华), Chao Liu(刘超), Hu Chen(陈虎)

Chin. Phys. B . 2018, 27(1): 018703. **doi:** 10.1088/1674-1056/27/1/018703

Enhancement in solar hydrogen generation efficiency using InGaN photoelectrode after surface roughening treatment with nano-sized Ni mask

Tao Tao, Zhi Ting, Li Ming-Xue, Xie Zi-Li, Zhang Rong, Liu Bin, Li Yi, Zhuang Zhe, Zhang Guo-Gang, Jiang Fu-Long, Chen Peng, Zheng You-Dou

Chin. Phys. B . 2014, 23(9): 096203. **doi:** 10.1088/1674-1056/23/9/096203

Mechano-chemical selections of two competitive unfolding pathways of a single DNA i-motif

Xu Yue, Chen Hu, Qu Yu-Jie, Artem K. Efremov, Li Ming, Ouyang Zhong-Can, Liu Dong-Sheng, Yan Jie

Chin. Phys. B . 2014, 23(6): 068702. **doi:** 10.1088/1674-1056/23/6/068702

Controllable synthesis of high aspect ratio $Mg_2B_2O_5$ nanowires and their applications in reinforced polyhydroxyalkanoate composites

Mo Zhao-Jun, Chen Jin-Peng, Lin Jing, Fan Ying, Liang Chun-Yong, Wang Hong-Shui, Xu Xue-Wen, Hu Long, Tang Cheng-Chun

Chin. Phys. B . 2014, 23(5): 056201. **doi:** 10.1088/1674-1056/23/5/056201

Probing conformational change of T7 RNA polymerase and DNA complex by solid-state nanopores*

Xin Tong(童鑫)[1], Rui Hu(胡蕊)[1], Xiaoqing Li(李晓晴)[1], and Qing Zhao(赵清)[1,2,†]

[1] *State Key Laboratory for Mesoscopic Physics and Electron Microscopy Laboratory, School of Physics, Peking University, Beijing* 100871, *China*
[2] *Collaborative Innovation Center of Quantum Matter, Beijing* 100084, *China*

(Received 19 June 2018; revised manuscript received 14 August 2018; published online 19 October 2018)

Proteins are crucial to most biological processes, such as enzymes, and in various catalytic processes a dynamic motion is required. The dynamics of protein are embodied as a conformational change, which is closely related to the flexibility of protein. Recently, nanopore sensors have become accepted as a low cost and high throughput method to study the features of proteins. In this article, we used a SiN nanopore device to study the flexibility of T7 RNA polymerase (RNAP) and its complex with DNA promoter. By calculating full-width at half-maximum (FWHM) of Gaussian fits to the blockade histograms, we found that T7 RNAP becomes more flexible after binding DNA promoter. Moreover, the distribution of fractional current blockade suggests that flexibility alters due to a breath-like change of the volume.

Keywords: solid-state nanopore, T7 RNA polymerase, conformational change, protein flexibility

PACS: 87.80.Nj, 62.23.St, 87.15.–v **DOI:** 10.1088/1674-1056/27/11/118705

1. Introduction

A solid-state nanopore sensor is an effective method to obtain information about single biomolecules.[1–4] The idea of nanopore sensing comes from the Coulter-counter method to evaluate particles in solution.[2–4] In a container full of electrolyte, the container is divided into two chambers by an insulating chip with a small pore. When a molecule is translocating through the pore under an electric field, the conductance of the system will decrease, and the decrease is related to the geometry and charge of the molecule. A nanopore sensor works by analyzing the change of the current caused by molecule translocation across the nanopore. In previous research, a solid-state nanopore sensor has been shown to be a reliable and accurate method for detecting nucleic acids,[5–12] protein,[13–16] and synthetic structures.[17–22]

Proteins are crucial to most biological processes, such as enzymes, and they are dynamic during the catalytic process. The dynamics of protein are reflected in its conformational change, which is caused by local and collective thermal motion of atoms and chains. Many studies have shown that the conformational change of a protein highly influences its function.[23–28] Many techniques have been used to probe protein flexibility, such as Fourier transform infrared spectroscopy (FTIR), circular dichroism (CD),[28] x-ray crystallography,[29] and nuclear magnetic resonance (NMR).[30] Nevertheless, in those techniques, chemical modification or crystallization of protein is needed, which may influence the structure of the protein and lead to inaccurate structural information being obtained. Compared to other methods, a solid-state nanopore can gauge the label-free protein in solvent, similar to intracellular environment, and it can also analyze protein in real time. Recently, Waduge *et al.* demonstrated that the breadth of current blockades increases with more flexible proteins by measuring a set of proteins.[31,32] A protein with larger flexibility can have more possible configurations when it passes through the nanopore, thus it will provide wider distributions of current blockages, resulting in wider full-width at half-maximum (FWHM) values from Gaussian fits to the current blockade histograms. In this method, FWHM values obtained from Gaussian fits to the current blockade histograms could be used an indicator of protein flexibility. A larger FWHM value suggests higher flexibility of the protein.

T7 RNA polymerase (RNAP) is one of the ideal models for studying the interaction between DNA promoter and polymerase because it can easily form a tight binary complex with DNA promoter.[33–36] T7 RNA polymerase is a DNA-dependent RNA polymerase which consists of a single polypeptide chain and has a molecular weight of 99 kDa. As Fig. 1(a) shows, T7 RNAP is constituted by N-terminal domain (8–325), thumb sub-domain (326–411), palm sub-domain (421–449, 528–553 and 785–879), palm insertion module (450–527), fingers sub-domain (554–739 and 759–784), specificity loop (740–769), and extended foot module (838–879).[37] The N-terminal domain is flexible in solution, which interacts with upstream regions of promoter and RNA to begin the catalysis.[38] The thumb sub-domain is a poorly ordered part of RNAP, and affects the affinity of template DNA towards T7 RNAP.[35,39] The palm sub-domain is dis-

*Project supported by the National Natural Science Foundation of China (Grant Nos. 51622201, 91733301, and 61571015).
†Corresponding author. E-mail: zhaoqing@pku.edu.cn
© 2018 Chinese Physical Society and IOP Publishing Ltd

ordered in electron density maps, and directly participates in catalysis.[40,41] The fingers sub-domain is comparatively ordered, and supports the specificity loop, which is involved in recognizing promoter.[42] The palm insertion module is a 77 residues insertion in the palm sub-domain, working as a switch to shut down the channel of binding nucleic acid with its conformation changing in this process.[43] The extended foot module interacts with incoming rNTPs and promoter to continue the transcription, and its flexibility in solution changes after forming complex.[40,44]

In the binding process, promoter sequence-specific recognition is accomplished by the specificity loop. Meanwhile, at position −17 to −13, AT-rich promoter sequence is recognized by a loop in the N-terminal domain, which proceeds the transcription. DNA strands are then melted by the fingers sub-domain and remain as single-stranded until the position +1, and the complex is prepared during the transcription at the active site of the palm sub-domain.[33,37,45] The crystal structure of the polymerase shows the diameter of about 8 nm for T7 RNA polymerase. In a solution of pH = 8.0, T7 RNAP will be negatively charged. Studying the flexibility of T7 RNA and its complex may reveal a more detailed understanding of the interaction between RNA polymerase and its promoter.

The static structure of T7 RNAP and its complex with DNA promoter has been already studied by using x-ray crystallography,[35,36] but the conformational change of T7 RNAP complex in solvent remains unclear. In this article, we take advantage of solid-state nanopore to probe T7 RNAP and its complex in solution. The translocation events of T7 RNAP and its complex are analyzed, and FWHM values from Gaussian fits of blockages are calculated, respectively. We find that compared to T7 RNAP, the FWHM value is larger in its complex, suggesting a larger flexibility of T7 RNAP complex, which means that the flexibility of T7 RNAP increases after binding DNA promoter. This increase may relate to the function changes of T7 RNAP after initiation. Our results further support that the flexibility change is due to a breath-like 70 nm^3 volume change.

2. Materials and methods

2.1. Nanopore fabrication

Nanopore chips were fabricated using double-sided polished silicon wafer chips with a thickness of 400 μm as the substrate. 2 μm silicon dioxide films were fabricated by thermal oxidation and 50 nm silicon nitrides were deposited by low pressure chemical vapor deposition on both sides of the silicon wafer. Reactive ion etching was then used to remove 30 nm SiN on one side. By standard dry and wet etching at the other side, a 40 μm×40 μm SiN window was created and a 20 nm SiN freestanding membrane remained at the center of the chip, as Fig. 1(b) shows. Then 8–10 nm nanopores were drilled on the freestanding SiN membrane with transmission electron microscope (TEM) (FEI, Tecnai F30) operated at 300 kV, as Fig. 1(c) shows. Before the experiments, a piranha solution and plasma cleaning were carried out to keep the chips hydrophilic.

2.2. Sample preparation

To obtain the RNAP–DNA complex, we chose a 22 bp ds-DNA fragment as promoter for T7 RNAP (New England Biolabs, Inc., America) to form the complex. In the promoter, the nontemplate sequence was

5'-TAATACGACTCACTATAGGGAG-3'.

An extra 5'-GGGAG-3' at positions through +1 to +5 was added to form the complex. Using PCR, we synthesized the ds-DNA fragment and checked it by gel electrophoresis (2% Argarose Gel, 120 V, 20 min, 100 bp DNA maker). The result is shown in Fig. S1 of the supporting information. To make the RNAP–DNA complex, we used a reaction environment containing pH = 8, 2 mM MgCl, 20 mM Tris, 51 μM T7 RNAP, and 93.6 μM DNA promoter. Then the mixture was incubated for 10 min at 37 °C to form the RNAP–DNA complex.

2.3. Nanopore experiment

In the nanopore experiment, the nanopore chip was immobilized among two pieces of custom-designed Teflon chambers, which were filled with buffer (0.15 M NaCl and 10 μM HEPES at pH = 8.0). Two Ag/AgCl electrodes connected to each chamber were linked to the Axopatch 200B (Molecular Devices, Inc., Sunnyvale, CA), which provided a constant voltage bias between the two chambers and amplified the ionic current signal for recording in real time. The prepared T7 RNAP samples were added into one of the chambers with a concentration of 51 nM at room temperature. Then 60–140 mV voltage was applied to drive the T7 RNAP or its complex passing through the pore (Fig. 1(b)). The current signal was filtered by a 100 kHz low-pass Bessel filter in the Axopatch 200B. The data was then acquired at a sample rate of 250 kHz by Axon Digidata 1440 A digitizer and pClamp10 software. The signal was analyzed by a custom-made Matlab program to find the translocation events of passing molecules and extract the parameters of the current signal.

3. Results and discussion

To study the conformational change of T7 RNAP binding DNA promoter, three series of nanopore experiments were carried out where T7 RNAP sample only, DNA promoter only, and T7 RNAP complex with DNA promoter were used as three sets of target molecules, respectively. A schematic of

the experimental setup is shown in Fig. 1(b), as the negatively charged sample molecules are translocated through the drilled SiN nanopore under an electric field. The typical TEM-drilled SiN nanopore ($d \sim 10$ nm) is shown in Fig. 1(c), which is only a little bit larger than the T7 RNAP molecule.

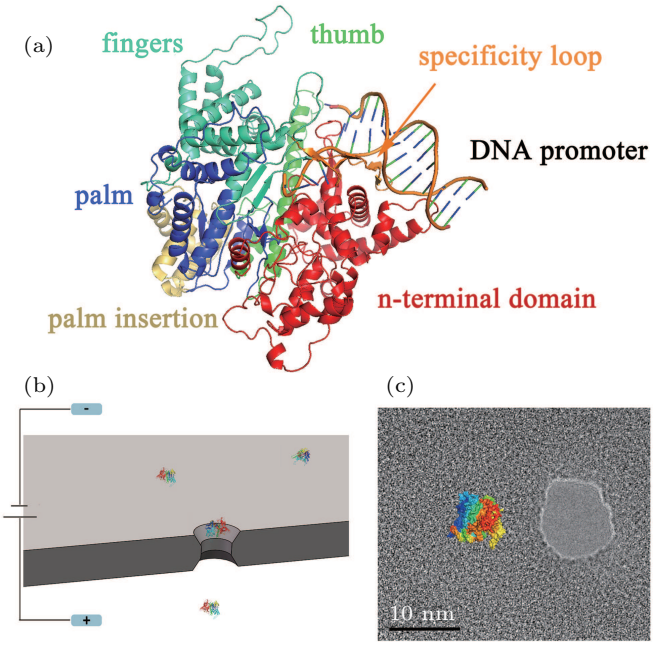


Fig. 1. (color online) (a) PDB-based cartoon shows the structure of the T7 RNAP and complex with DNA promoter, which are colored by domain and module, with the N-terminal domain (red), the thumb (green), the palm (blue), the palm insertion module (yellow), the fingers (cyan), the specificity loop (orange). (b) Schematic of the nanopore sensor used in this work. A SiN membrane separates the electrolyte-filled space into two chambers which are connected by a nanoscale pore. An applied voltage between the electrodes generates an electrical field to drive the protein crossing the pore. (c) TEM image of a 10 nm nanopore used in this work, and a size comparison with T7 RNAP.

The current baseline through the nanopore is rather smooth (Fig. 2(a)) with low noise (Fig. S2 of the supporting information). The DNA promoter is not detected through nanopore experiments due to its small size and limited temporal resolution (Fig. 2(b)). Once the T7 RNAP sample is added into the nanopore chamber, a large number of translocation events are observed as conductance dropping, as shown in Fig. 2(c). From previous reports, one can obtain the volume of the detected molecules through nanopore experiments by using the following equation:[46,47]

$$\Delta G = \frac{\sigma \gamma \Lambda}{(h_{\text{eff}} + 0.8d)^2}, \tag{1}$$

where the average conductance blockage ΔG can be obtained from the translocation event density map of conductance blockage versus dwell time, σ is the conductivity of the solution, γ is the shape factor of the detected molecule, Λ is the volume of the detected molecule, h_{eff} is the effective thickness of the nanopore, and d is the average diameter of the nanopore. Equation (1) demonstrates the correlation between the average conductance blockage ΔG from nanopore experiments of detected molecules and the parameters of the nanopore. Therefore, the volume of T7 RNAP can be calculated by the above expression if all of the other parameters are known. From the T7 RNAP translocation event density map of conductance blockage versus dwell time (Fig. 2(e)), ΔG is 2.8 nS. From the experiment conditions (salt concentration), σ is 2.3 S·m^{-1}. For sphere-like molecule such as T7 RNAP, $\gamma = 1$. The diameter of nanopore d can be obtained from TEM image, which is 10 nm for our nanopore. The effective thickness of the nanopore is obtained by a control experiment with a well-known BSA protein molecule translocation using the same nanopore (Fig. S3 of the supporting information). The calculated h_{eff} is approximately 7.2 nm (detailed calculation process can be found following Fig. S3 of the supporting information). After finding the other parameters, according to Eq. (1), the diameter of T7 RNAP is calculated to be 8.1 nm, in good agreement with the value obtained from x-ray crystallography,[35] which further proves the validity of nanopore experiments and calculation method.

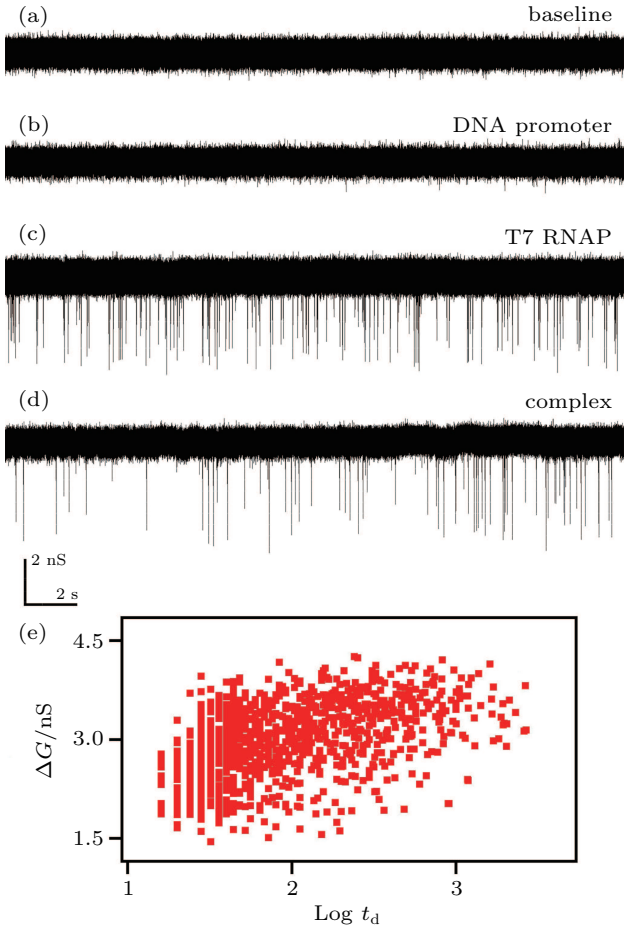


Fig. 2. (color online) Current traces captured by Axon 200B for electrolyte (a), DNA promoter (b), T7 RNAP (c), and complex (d) obtained by a 10 nm nanopore in a condition of 0.15 M NaCl, pH = 8, and applied voltage of 100 mV. (e) Scatter plot of ΔG vs log dwell-times (t_d) for T7 RNAP with a 10 nm nanopore and applied voltage 100 mV.

The bias voltage is the primary parameter that one can alter in nanopore experiment and offers the electric field force

which drives the protein through the nanopore. Obviously, a larger bias can lead to a higher translocation speed of the protein across the pore, which will be reflected by shorter time durations of translocation events. Meanwhile, a larger external electric field can also cause a higher capture rate of translocating molecules.[48] Figures 3(a)–3(c) show three time duration histograms of T7 RNAP blockage events under three different voltage biases (60 mV, 100 mV, 140 mV). One can see that the average time duration becomes shorter under larger voltage bias, indicating that the blockage events are caused by smooth translocation of T7 RNAP molecules. The capture rate shows a linear increase as a function of voltage when the voltage is smaller than 100 mV (Fig. 3(d)). However, the capture rate decreases when the voltage bias is larger than 100 mV, because the time duration of translocation event is too short to be identified under larger voltage due to limited temporal resolution (4 μs) in normal nanopore experimental setup. The bandwidth of the amplifier circuit limits the resolution of duration, and shorter event under larger voltage (> 100 mV in this case) cannot be detected due to the limited temporal resolution. For voltage bias lower than 100 mV, the event duration is sufficiently long for current blockage analysis, which can provide a good capture rate for data analysis.

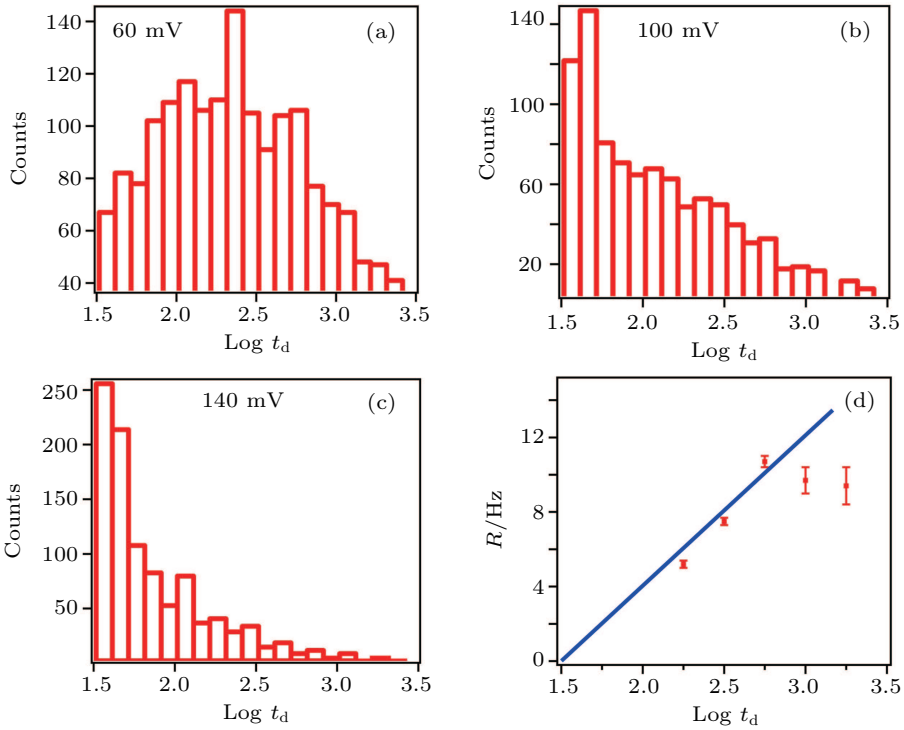


Fig. 3. (color online) Histogram of log dwell-time (t_d) for T7 RNAP in certain applied voltages of (a) 60 mV, (b) 100 mV, and (c) 140 mV. (d) The capture rate as a function of applied voltage for T7 RNAP. The blue straight line is obtained by binomial fitting of first 3 points and coordinate zero.

After analyzing the translocation events of T7 RNAP molecules, we did nanopore experiments with T7 RNAP complex. Figure 2(d) shows the current trace of translocation events of complex with T7 RNAP and DNA promoter. Figures 4(a) and 4(b) show the contour plots of T7 RNAP and complex translocation events under bias 100 mV, respectively. In both contour diagrams, the fraction blockage is gathered at 0.4, indicating that binding DNA has little impact on size change of T7 RNAP. This character is also found in T7 RNAP and complex structures from x-ray crystallography.[35,36] In the complex contour diagram (Fig. 4(b)), the fraction blockage distribution of translocation events is more dispersed than that in T7 RNAP (Fig. 4(a). In particular, more events appear in the area with a smaller blockage that we consider T7 RNAP as a shrink state. Meanwhile, time duration is centered at 100 μs in both cases.

To probe the flexibility of these two samples, we calculate the FWHM values from Gaussian fits to the fraction blockage of translocation events of T7 RNAP and complex (Figs. 4(c) and 4(d)). From the histogram, it is evident that the FWHM of complex is larger than that of T7 RNAP. The T7 RNAP sample shows FWHM of 0.179, and the complex sample shows FWHM of 0.207. From previous study,[31,32] larger FWHM suggests a higher flexibiliy of translcoating molecules. The larger FWHM of the complex sample suggests a greater flexibility in T7 RNAP binding DNA promoter complex. This difference is contributed by events with fraction blockage in the range of 0.3 to 0.35. Compared to the most probable range of 0.4–0.45 (Figs. 4(c) and 4(d)), there is a quarter diminution of blockage. If we regard all of those events as a sphere across the pore, by using Eq. (1), we could easily calculate the volume change in complex to be about one fourth, which is

70 nm^3. We did the same experiment using another nanopore ($d \sim 12$ nm). Very similar results were found that FWHM increases from Gaussian fits to the fraction blockage of translocation events in T7 RNAP and DNA complex samples (Fig. S4 of the supporting information).

From the increase of FWHM (Figs. 4(c) and 4(d)), we can obtain that T7 RNAP becomes more flexible after binding DNA promoter to form complex. This increase comes from extension of distribution of events blockage, which suggests that the complex is much easier to reach a shrink state. In the binding process, DNA promoter activates the T7 RNAP to open this state. Therefore, the flexibility of the complex performs like breathing, which has two states alternating with time. This breath takes 70 nm^3 volume change of the T7 RNAP, which is too large if only module is involved. Consequently, domain and sub-domain participate in this conformational change, while thumb and fingers sub-domains may impact the promoter in the whole binding process.

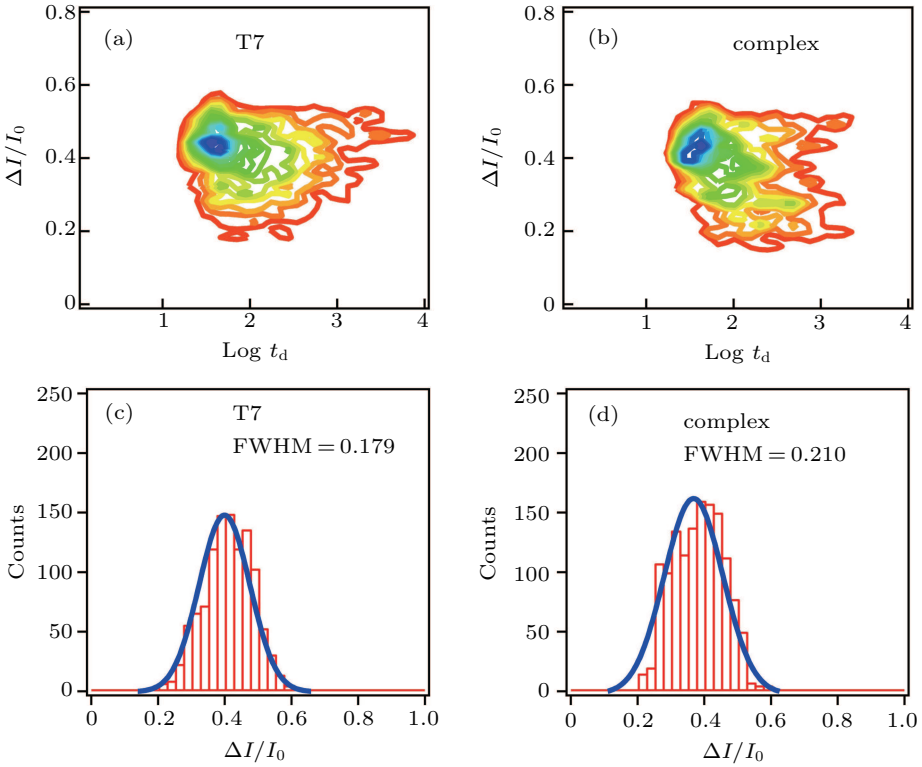


Fig. 4. (color online) Color contour plots of $\Delta I/I_0$ vs log dwell-time (t_d) for T7 1142 events (a) and complex 1214 events (b) with a 10 nm nanopore and applied voltage of 100 mV. Histograms of $\Delta I/I_0$ for T7 (c) and complex (d) events. The histograms are fitted with Gaussian distributions (blue curves).

4. Conclusion and perspectives

In summary, we used SiN nanopore sensor to probe T7 RNAP and its complex with DNA promoter. Duration histograms of T7 RNAP under different bias voltages indicate smooth translocation of detected molecules. Furthermore, the FWHM values of Gaussian fits to the blockade histograms of T7 RNAP and complex translocation events indicate that the complex is more flexible in our experiment. Our analysis suggests that T7 RNAP's flexibility changes after binding DNA promoter and this dynamic change activates a state that decreases the volume of T7 RNAP. Moreover, we calculated the decreased volume of T7 RNAP and have supposed that this decrease is caused by major component of T7 RNAP, such as thumb and fingers sub-domains. Our findings may be helpful to reveal the interaction of T7 RNAP and its promoter, and it gives an insight into the protein activity variations caused by conformational change.

References

[1] Li J, Stein D, McMullan C, Branton D, Aziz M J and Golovchenko J A 2001 *Nature* **412** 166
[2] Dekker C 2007 *Nat. Nanotech.* **2** 209
[3] Venkatesan B M and Bashir R 2011 *Nat. Nanotech.* **6** 616
[4] Haque F, Li J H, Wu H C, Ling X J and Guo P X 2013 *Nano Today* **8** 56
[5] Li J, Gershow M, Stein D, Brandin E and Golovchenko J A 2003 *Nat. Mater.* **2** 611
[6] Storm A J, Chen J H, Zandbergen H and Dekker C 2005 *Phys. Rev. E* **71** 051903
[7] Storm A J, Storm C, Chen J H, Zandbergen H, Joanny J F and Dekker C 2005 *Nano Lett.* **5** 1193
[8] Wanunu M, Sutin J, McNally B, Chow A and Meller A 2008 *Biophys. J.* **95** 4716
[9] Wanunu M, Sutin J and Meller A 2009 *Nano Lett.* **9** 3498
[10] Henley R Y, Ashcroft B A, Farrell I, Cooperman B S, Lindsay S M and Wanunu M 2016 *Nano Lett.* **16** 138
[11] Kowalczyk S W, Hall A R and Dekker C 2010 *Nano Lett.* **10** 324
[12] Alibakhshi M A, Halman J R, Wilson J, Aksimentiev A, Afonin K A and Wanunu M 2017 *ACS Nano* **11** 9701
[13] Fologea D, Ledden B, McNabb D S and Li J 2007 *Appl. Phys. Lett.* **91** 539011

[14] Yusko E C, Johnson J M, Majd S, Prangkio P, Rollings R C, Li J, Yang J and Mayer M 2011 *Nat. Nanotech.* **6** 253

[15] Larkin J, Henley R Y, Muthukumar M, Rosenstein J K and Wanunu M 2014 *Biophys. J.* **106** 696

[16] Yusko E C, Bruhn B R, Eggenberger O M, Houghtaling J, Rollings R C, Walsh N C, Nandivada S, Pindrus M, Hall A R, Sept D, Li J, Kalonia D S and Mayer M 2017 *Nat. Nanotech.* **12** 360

[17] Kowalczyk S W, Hall A R and Dekker C 2010 *Nano Lett.* **10** 324

[18] Raillon C, Cousin P, Traversi F, Garcia-Cordero E, Hernandez N and Radenovic A 2012 *Nano Lett.* **12** 1157

[19] Ivankin A, Carson S, Kinney S R and Wanunu M 2013 *J. Am. Chem. Soc.* **135** 15350

[20] Bell N A W and Keyser U F 2015 *J. Am. Chem. Soc.* **137** 2035

[21] Plesa C, Ruitenberg J W, Witteveen M J and Dekker C 2015 *Nano Lett.* **15** 3153

[22] Sze J Y Y, Ivanov A P, Cass A E G and Edel J B 2017 *Nat. Commun.* **8** 1552

[23] Teague S J 2003 *Nat. Rev. Drug Discov.* **2** 527

[24] Radivojac P, Obradovic Z, Smith D K, Zhu G, Vucetic S, Brown C J, Lawson J D and Dunker A K 2004 *Protein Sci.* **13** 71

[25] Allen T W, Andersen O S and Roux B 2004 *J. Gen. Physiol.* **124** 679

[26] Kokkinidis M, Glykos N M and Fadouloglou V E 2012 *Adv. Protein Chem. Struct. Bio.* **87** 181

[27] Bershtein S, Mu W, Serohijos A W, Zhou J and Shakhnovich E I 2013 *Mol. Cell* **49** 133

[28] Celej M S, Montich G G and Fidelio G D 2003 *Protein Sci.* **12** 1496

[29] Fraser J S, van den Bedem H, Samelson A J, Lang P T, Holton J M, Echols N and Alber T 2011 *Proc. Nat. Acad. Sci. USA* **108** 16247

[30] Park S J, Borin B N, Martinez-Yamout M A and Dyson H J 2011 *Nat. Struc. Mol. Biol.* **18** 537

[31] Waduge P, Hu R, Bandarkar P, Yamazaki H, Cressiot B, Zhao Q, Whitford P C and Wanunu M 2017 *ACS Nano* **11** 5706

[32] Hu R, Rodrigues J V, Waduge P, Yamazaki H, Cressiot B, Chishti Y, Makowski E, Shakhnovich E, Zhao Q and Wanunu M 2018 *ACS Nano* **12** 4494

[33] Ujvári A and Martin C T 1996 *Biochemistry* **35** 14574

[34] Jia Y and Patel S S 1997 *Biochemistry* **36** 4223

[35] Sousa R, Chung Y J, Rose J P and Wang B C 1993 *Nature* **364** 593

[36] Cheetham G M, Jeruzalmi D and Steitz T A 1999 *Nature* **399** 80

[37] Jeruzalmi D and Steitz T A 1998 *EMBO J.* **17** 4101

[38] Muller D K, Martin C T and Coleman J E 1988 *Biochemistry* **27** 5763

[39] Kim Y, Eom S H, Wang J, Lee D, Suh S W and Steitz A 1995 *Nature* **376** 612

[40] Mookhtiar K A, Peluso P S, Muller D K, Dunn J J and Coleman J E 1991 *Biochemistry* **30** 6305

[41] Steitz T A 1993 *Curr. Opin. Struct. Biol.* **3** 31

[42] Raskin C A, Diaz G, Joho K and McAllister W T 1992 *J. Mol. Biol.* **228** 506

[43] Holm L and Sander C 1994 *Proteins* **19** 165

[44] Gardner L P, Mookhtiar K A and Coleman J E 1997 *Biochemistry* **36** 2908

[45] Chen Y C and Jeng S T 2000 *Biosci. Biotechnol. Biochem.* **64** 1126

[46] Han A, Creus M, Schürmann G, Linder V, Ward T R, Rooij N F and Staufer U 2008 *Anal. Chem.* **80** 4651

[47] Ito T, Sun L and Crooks R M 2003 *Anal. Chem.* **75** 2399

[48] Smeets R M, Kowalczyk S W, Hall A R, Dekker N H and Dekker C 2009 *Nano Lett.* **9** 3089